ATLAS Internal Note

LARG-NO-075

26 May 1997

LIQUID ARGON ELECTROMAGNETIC CALORIMETER FOR ATLAS. ABSORBERS OF ENDCAP WITH CONSTANT LEAD THICKNESS : THERMAL EXPANSION COEFFICIENT

Pablo Romero

Universidad Autónoma de Madrid

Abstract

This note describes the thermal analysis performed on the absorbers of ATLAS Electromagnetic Calorimeter End Cap with constant lead thickness, using Finite Elements Method. The aim of this analysis is obtaining the overall thermal expansion coefficient for the sandwich configuration - consisting of stainless steel, pre-preg and lead layers-, ans so that could be used as the key value to calculate the flat developed shape of the absorber as well as for its different layers: lead, steel and prepreg contours. Besides of this application, the coefficient here calculated can be used to create the surfaces of bending knives and curing knives, critical items for the absorbers tooling design.

Contents

1 ABSORBERS GEOMETRY

The absorbers geometry is based on Reference [1]. All the geometrical parameters (number of waves, wave angles, folding fillet radius, etc.) have been extracted from the IGES files corresponding to the above mentioned report. The sandwich configuration has several layers, which follow the stacking sequence: stainless steel + pre-preg + lead + pre-preg + stainless steel.

In relation to the contour of absorbers, those have built starting from the projectivity cuts defined in the drawings [3].

The most significant data for the thermal analysis are the thicknesses of layers, which have been stablished as follows:

for the lead

- Outer absorber: 1.7 mm
- Inner absorber: 2.2 mm

while for steel and prepreg the thicknesses are:

- Steel: 0.2 mm
- Pre-preg: 0.15 mm

These values translate into the overall thickness for the sandwich:

- Outer absorber: 2.4 mm
- Inner absorber: 2.9 mm

2 ABSORBERS MATERIAL

All the material properties employed on the finite element model are those defined in the Reference [2]:

.	$E(+20^0C)(MPa)$	$E(-186^0C)(MPa)$	ν	$\alpha(mm/mm^0C)$
$LEAD$	13734	15382	0.42	$2.74E-05$
$ST.STEEL$	186390	208757	0.31	$1.37E-05$
$PRE-PREG$	19620	19620	0.15	$1.05E-05$

Notice that:

- the plastic behaviour of the lead has been modelized too (see fig.0a)
- all the materials are assumed isotropic, including the pre-preg.
- The thermal coefficient has been taken as a mean value between (-186^{0}C, 20^{0}C) interval (see fig.0b)
- The elastic modulus has been considered as at cryogenic temperature as at room temperature

3 FINITE ELEMENTS CODE

The utilized Finite Elements Code is a general purpose software named ABAQUS/Standard V.5.4

Some of most powerful capabilities of this code that have allowed to perform the requested mechanical and thermal analysis are the following ones:

- Modelling either composite or laminate shells.
- Dealing with non linear material properties, such as plasticity.
- Dealing with non geometric linearities, such as large displacements.

4 ABSORBERS ANALYSIS

4.1 The coordinate system

The global coordinate system of the model is presented on figure 1. The beam axis is number 1 (OX), the axis parallel to the waves is number 2

(OY) and the vertical axis is number 3 (OZ).

4.2 Shell-Solid Modelling

The advantages of this model in comparison to the either shell modelling or solid modelling were deeply discussed in the Reference [2]. In few words, the shell solid modelling simulates the best the behaviour of prototipe tests, as transversal as parallel deformations to the waves. This kind of model meshing, with together the plastic behaviour of lead, gave the most accurate results as was checked from the above mentioned note.

The optimum meshing size have been stablished after some trials, in order to have a compromise between computer model size -number of degrees of freedom- and accuracy.

.	*Shells*	*Solids*	*d.o.f.*
Inner	861	7413	37884
Outer	2301	17938	99840

The shell-solid transition zone is modelized with multipoint constraints (MPC). Be careful with these MPC, which actually work as algebraic equations added to the matrix system , because they might be a source of geometrical non linearities. In fact, these constraints may be quite general, involving nonlinear and nonhomogeneous equations. In our case, the selected MPC and its associated equations they all are conceptually nonlinear constraints, but as being used in a geometrically linear analysis (small strain and displacements field), the MPC are linearized.

4.3 Isostatic Boundary Conditions.

The model will have to undergo a warming up from -186^{0}C to 20^{0}C (room temperature), without applying mechanical loads like gravity (the absorber weight itself) or thrust (due to inmersing the absorber in argon liquid).

Keep on mind the objective of this analysis is determining the thermal expansion coefficient for the whole sandwich configuration of absorbers. A

hyperestatic support condition must be avoided. Otherwise, that could give rise to stresses and strains due to the boundary conditions themselves.

Therefore, the calculated stress field is caused by the different materials that the the sandwich is made up of. If the model would consist of the same material only, with together the isostatic boundary conditions, the stress and strain field should be null (almost cero because the finite element method is an approximate method).

All boundary conditions are plotted on figure 1. In order to prevent the model from rigid body mouvements, one node has also fixed its three displacements u_x,u_y and u_z.

4.4 Uniform Thermal Load.

As it was advanced in the previous paragraph, a incremental thermal load of 206^0C is applied to the whole model. A uniform temperature field is assumed as initial condition (-186^0C) as well as final condition (20^0C). The steady condition at the end of the thermal increment is calculated. The non steady states along the warming up is neither considered nor simulated.

Our only purpose is obtaining a value (the thermal coefficient) that characterizes the best possible the behaviour of the absorbers from cold condition to room temperature, but not going into details about how this evolution is. We are not interested in the path, but just in the initial and final states.

4.5 Real Evolution Considerations

The analysis here reported uses the absorber dimensions/geometry at cold temperature as the initial condition; this design geometry has been defined by phisycists. Then, a thermal load is applied to reach the room temperature, which is the final condition. Notice that at initial condition there are no stresses, but they do rise as the temperature increases.

However, the real evolution behaves in an opposite direction: at room temperature, the sandwich have been piled up, bended and cured. Not considering the interlayer stresses caused by the curing cycle, we can assume the stress field is null at room temperature. After putting the absorber into the

cryostat and cooling down the whole End Cap to the final liquid argon temperature (-186^{0}C), the absorbers should adopt its design geometry, and at the same time, a stress field appears along its layers, even the lead reaching its plastic behaviour.

So, a question comes up: How can the simulated path be matched against the real evolution? Before continuing our reasoning, some analysis features should be pointed out:

- The analysis is static, as it already was justified in paragraph 4.4. We did not perform a dynamic analysis. If the model would have actually been linear, the hypothesis of assuming the final state independent of the path would have been completely right. However, a non linear effect has been introduced in the model by means of lead plasticity. Therefore, the final condition does depends on how this state is reached, and the solution must be obtained by following the actual loading sequence.

- A nonlinear static analysis requires the solution of nonlinear equilibrium equations, for wich Abaqus uses Newtons'method. The solution is obtained as a series of increments, with iteration within each increment to obtain equilibrium.

- We always are in the small strain range, and in the small displacements range as well. However the non linearity is present in the model due to the plastic behaviour of the lead. That involves the stiffness matrix depends on the strain field, though it still remains independent of the displacement field.

As consecuence of all these features, we can assume that:

- if the thermal load from cold condition to the warmed one has the same profile than for the reverse evolution - in our case the real evolution - , the stress, strain and displacement field would be coincidents. This concept is showed in figure 2.b: the stress ,strain and displacements field at point B (final state of our unrealistic simulation) must be the same than for those at point D (final state of the real process). Also, the loading sequence should be monotonous increasing w.r.t. time (see figure 2.a) , without peaks/valleys.

- in order to match the real evolution against the simulation here reported, the material properties should be taken at cold temperature, though for the simulation the final state is at room temperature.

What do all the above discussions mean? The results here calculated can be processed to get the warmed shape by only adding the displacement field u_d to the cold geometry. For the reverse calculation, if the same thermal load profile is applied to the warmed geometry, the subsequent cold geometry should coincide with the previous one.

4.6 Results Analysis

The figures 3 and 4 show the deformed (red color, at room temperature) and undeformed shape (blue color, at cryogenic temperature) for both absorbers, being displayed the deformed one with a magnification factor of 20. The embedded values on the contour area are the thermal coefficients along different locations, as it will be explained in the next paragraph.

From a qualitative point of view, the shape agrees with the prototype tests. Notice that in those areas whose cross sections are longer - where the waves have acute angles- the expanded length is longer too, and because of that the warmed geometry adopts this twisted and asymmetric shape.

4.6.1 Spatial Distribution of Thermal Coefficient

The following procedure has been conducted to evaluate the thermal expansion coefficient:

- Some characteristic curves were taken from the cold geometry, and their lengths were measured (Lc). In our case, these curves were: the bending lines, the straight lines on the wave surfaces, some cross sections perpendicular to the waves direction, as well as the boundary curves coming from the projectivity cuts.
- Adding the displacements provided by the thermal analysis to the cold geometry. This way, the transformed curves at room temperature are obtained and subsequentelly measured (Lh).
- The thermal coefficient (mm/mm^{0}C) is calculated by means of the expression:

$$\alpha = \frac{Lh - Lc}{LcAT}$$

AT = 206 ^{0}C, the incremental thermal load.

along different locations on the surfaces. The results are summarized in figures 3.a and 4.a : the embedded values on the contour area mean the thermal coefficients along different locations, corresponding, for the inner absorber, those of the middle row to parallel direction to the waves and those of upper and lower row to perpendicular direction to the waves (along the projectivity edges). For the outer one, replace row with column and the values will mean the same.

As you can check, there is no an uniform distribution of thermal coefficient on the surface. That could be indicative of different coefficients depending on the directions. The geometry of absorbers invites to account, at least, two main coefficients: transversal and parallel to the waves.

However, before accepting a non uniform thermal coefficient, we should spend a little more resources to discard some effects that might have not been taken into account.

- Meshing size. A finer mesh has been implemented on both absorber models, and the results did not improve significantly. In fact, the meshes here adopted are a compromise between computer resources and accuracy. So, this factor must be discarded as non uniformity cause.
- Displacement field. Seeing the figures 3 and 4, you can realize the thermal coefficient value is bigger as we get longer away from the fixed point (with its three displacements restricted). That means the coefficient is bigger on those areas whose displacements are bigger too. It seems to exist a cumulative effect, and could be indicative of the influence of the displacements on the thermal coefficient. Anyway, notice that the deformation field keeps on being small, as can be checked from the small increment for the angles with respect to its nominal value (figure 3.b).

Therefore, the small deformation hypothesis can be maintained, but not the small displacements one. Now, the geometric nonlinearities must not be linearized and the stiffness matrix does depend on the displacement field. The errors involved in such "small displacements" approximation were of the order of the strains and rotations compared to unity. So, the next step would

consist in removing the large displacements effect by means of implementing on the model the geometrical non linearity capability.

Performing again the analysis with this large displacements option, and following the same procedure for calculating the thermal coefficient values along the surface, the figures 5 are obtained. As expected, the spatial distribution of thermal coefficient is much more uniform than in the previous analysis, lying down all the values on an interval not bigger than 1.5 %. This deviation may come from roundness errors building the warmed geometry. Anyway, this deviation means 40 micrometers for a length of 1000 mm, which is the same order of magnitude than manufacturing tolerances.

As a summary, the calculated mean values are:

Outer absorber: α= 14.1x10e-6 mm/mm^{0}C

Inner absorber: α= 14.3x10e-6 mm/mm^{0}C

being the deviation with respect to the mean values not bigger than 1.5 %

4.6.2 Influence of the lead thickness on the thermal coefficient.

Once the uniformity of thermal coefficient has been demonstrated, the only variable influencing on the thermal coefficient is the lead thickness, as being fixed the remainder parameters: steel and pre-preg materials properties and layer thicknesses.

Therefore, it seems convenient to perform a parametric analysis, whose parameter is the lead thickness. The objective is estimating the sensivity of the thermal coeffcient as a function of the lead thickness. The figure 6 shows the thermal coefficient trend. Relative values are written rather than nominal values, so these ones are dependent of both lead thickness and absorbers geometry.

5 CONCLUSIONS

The main conclusion derived from the analysis here reported is the uniformity of thermal coefficient, not being the bending areas, in which the lead

stresses has reached beyond its yield limit, a source of "anisotropic effects".

That simplifies greatly the absorber shape developing: if the cold shape is developed, and next the thermal coefficient is used as scale factor to transform this flat shape, the final flat contour at room temperature should be the same than if the absorber warmed geometry had been obtained performing the thermal analysis and then this geometry had been developed. Keep on mind that this overall thermal coefficient is used to develop either lead layer, steel layer or pre-preg layer, ignoring the own thermal coeffcient for each material.

However, we must not ignore the approximation that has been introduced along the thermal coefficient estimation procedure. According to the paragraph 4.6.1, a geometrical non linearity had to be implemented on the model to demonstrate the uniformity of thermal coefficient, as well as to calculate its mean value. In the other hand, along the paragraph 4.5 the consequences of introducing non linearities on the model were discussed. The non linearity caused by the lead plasticity could be overcome making use of a reasoning based on the small displacements range, so that would allow to relate the real evolution with the results obtained in our "unrealistic" simulation.

But leaving the small displacements range and entering the geometrical non linearities, weakens our reasoning to match our simulation against the real evolution. Anyway, the goal of this large displacements option was commissioning the results rather than changing the analysis conceptually. In fact, in those areas close to the fixed point, the implementation of this option does not change significantly the obtained values. That does in those areas whose displacements are bigger, for which it seems to be a cumulative effect.

The large displacements option gets this cumulative effect removed and makes all the model be independent of the distance to the fixed point. Also, notice the small strain (or deformations) hypothesis has not been surpassed; remember the angles deformation is small compared to its nominal value.

If the isostatic boundary conditions would have been imposed in a different way, not existing areas so long away of the restricted points, likely it would not have been necessary to implement this large displacements option.

In short, we can assume and can expect that the non linearities (geometrical and material) does not affect the 4.5 paragraph reasoning in such extent than the sum of model error and all its induced approximation errors is bigger

than the error whose origin is manufacturing tolerances.

If the contours - either lead, steel or pre-preg- can be outcutted with an accuracy of +-0.1 mm, thus we cannot control more than 0.2 mm over 2 m, which is the characteristic length for the outer absorber plates. These values, taking a thermal range of 200^0C, translate into a error of 0.5x10e-6 mm/mm^{0}C. That means, for a thermal coefficient value of 14e-6, the manufacturing tolerances can involve a relative error of 5 %.

6 Application to the absorbers tooling design

As was described in the abstract, the main application of the thermal analysis here performed is calculating the developed flat contours for the differents layers of the absorbers (lead, steel and pre-preg) . Besides of this purpose, the analysis can be made use for obtaining the surfaces of the bending knives and curing knives, as it has been done in the references [4],[5],[6] and [7].

Taking the calculated thermal coefficient of the absorber as the key data, the primitive surface transforms into a scaled surface.

In the bending knives case, the starting surface is at cold temperature- cold geometry provided by the physicist group-, and the scale factors are the thermal coefficients listed in paragraph 4.6.1.

In the curing knives case, we cannot apply these values, so the real evolution goes from room temperat ure (20C) to curing temperature (approximately 120C). Therefore, a new analysis must be carried out, w hose changes with respect to what has been previously performed are focused in the material properties:

- Thermal coeffcients for the constituent materials. Now, the mean value is calculated between the (20 ^{0}C,120^{0}C) interval, taking as input the figure 0.b

- Elastic Modulus. Now, they are considered at room temperature (20C) instead of cryogenic temperature.

In relation to the modelling and meshing, we can make use of the previously defined. The same elements, all the parameters (size and degrees of freedom) as well as boundary conditions, are kept.

Performing the new analysis, the final results are the following:

Outer absorber: α= 17.86x10e-6 mm/mm^{0}C

Inner absorber: α= 18.16x10e-6 mm/mm^{0}C

7 References/Drawings

[1] ABS.YYY.00.DRa.3 :Creating IGES files of Absorbers. L. Martin, J.L. Gimenez. 13th May 1996

[2] Liquid Argon Electro Magnetic Calorimeter for Atlas: End Cap with Constant Lead Thickness Structural Analysis. Pablo Lopez Iturriaga. January 19, 1996

[3] GEN.ACP.00.ODa.1

[4] ABS.FLD.21.DRa.1. Creating IGES files of Inner Folding Knives. L. Martin. 12th June 1996

[5] ABS.FLD.22.DRa.1. Creating IGES files of Outer Folding Knives. L. Martin. 12th June 1996

[6] ABS.GLU.10.DRa.3. Creating IGES files of Outer Gluing Knives. L.Martin. 2nd October 1996

[7] ABS.GLU.20.DRa.2. Creating IGES files of Inner Gluing Knives. L.Martin. 2nd October 1996

8 Figures

Figure 0a: lead plasticity model

Figure 0b: Thermal expansion of lead. Data source: Cryogenic Data book UCRL-3421 P.87.

Figure 1a: boundary conditions and reference system for inner absorber

Figure 1b: boundary conditions and reference system for outer absorber

Figure 2a: Conceptual comparison of real and simulated evolutions. Thermal loading as function of time.

Figure 2a: Conceptual comparison of real and simulated evolutions. Stress,

strain and displacements fields as function of thermal load.

Figure 3a: top view of undeformed (at cold temperature,blue) and deformed (at room te mperature,red) shape of the inner absorber, with embedded thermal coefficient values along different locations. Small displacements analysis.

Figure 3b: front view of undeformed (at cold temperature,blue) and deformed (at ro om temperature,red) shape of the inner absorber . Small displacements analysis

Figure 4a: top view of undeformed (at cold temperature,blue) and deformed (at ro om temperature,red) shape of the outer absorber, with embedded thermal coefficient values along different locations. Small displacements analysis

Figure 5a: top view of undeformed (at cold temperature,blue) and deformed and deformed (at ro om temperature,red) shape of the inner absorber, with embedded thermal coefficient values along different locations. Non geometric linearity.

Figure 5b: top view of undeformed (at cold temperature,blue) and deformed and deformed (at ro om temperature,red) shape of the outer absorber, with embedded thermal coefficient values along different locations. Non geometric linearity.

Figure 6: sensivity of thermal coeffcient as function of lead thickness.

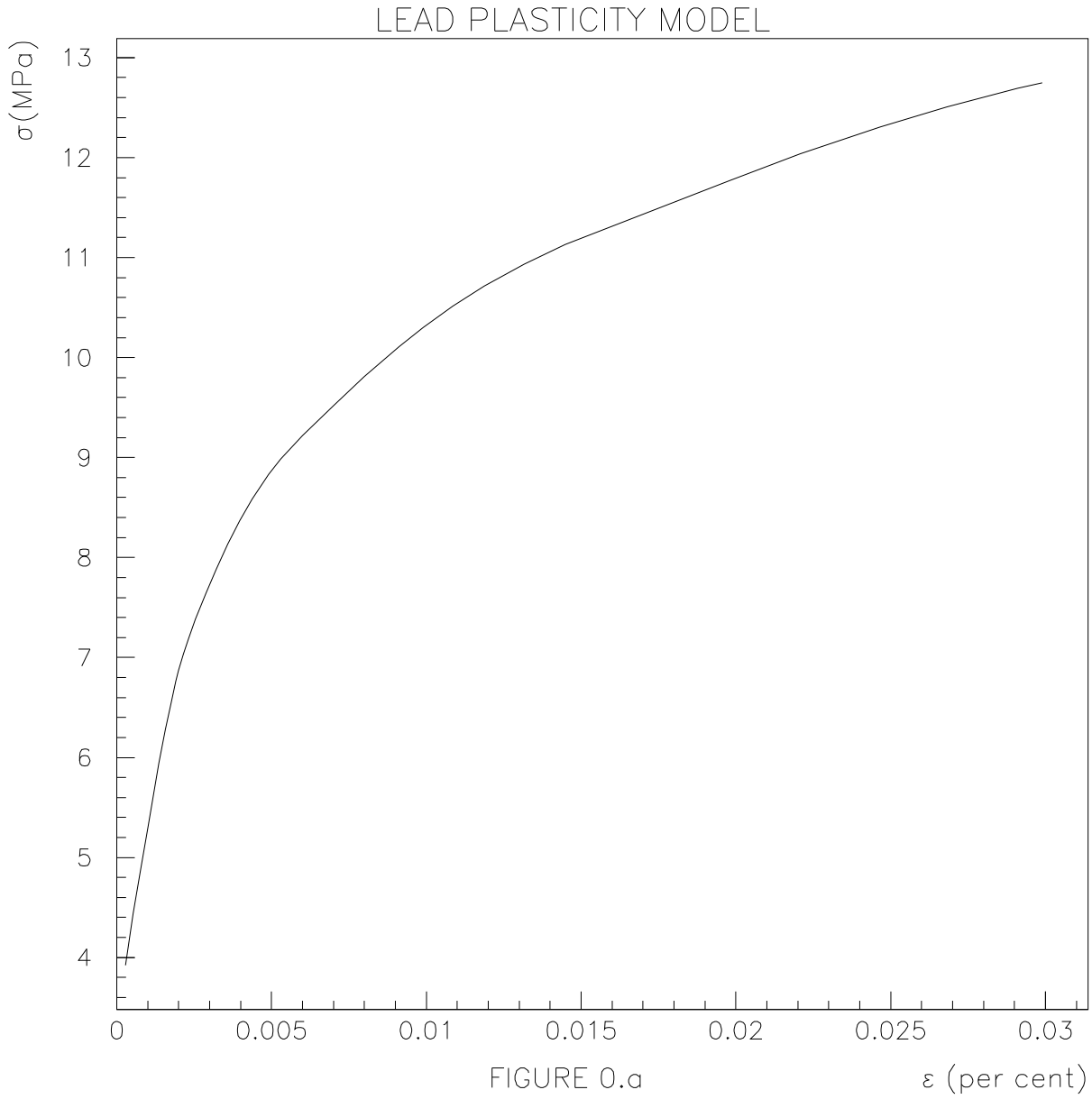
LEAD PLASTICITY MODEL
σ(MPa)
13
12
11
10
9
8
7
6
5
4
0
0.005
0.01
0.015
0.02
0.025
0.03
ε (per cent)

FIGURE 0.a

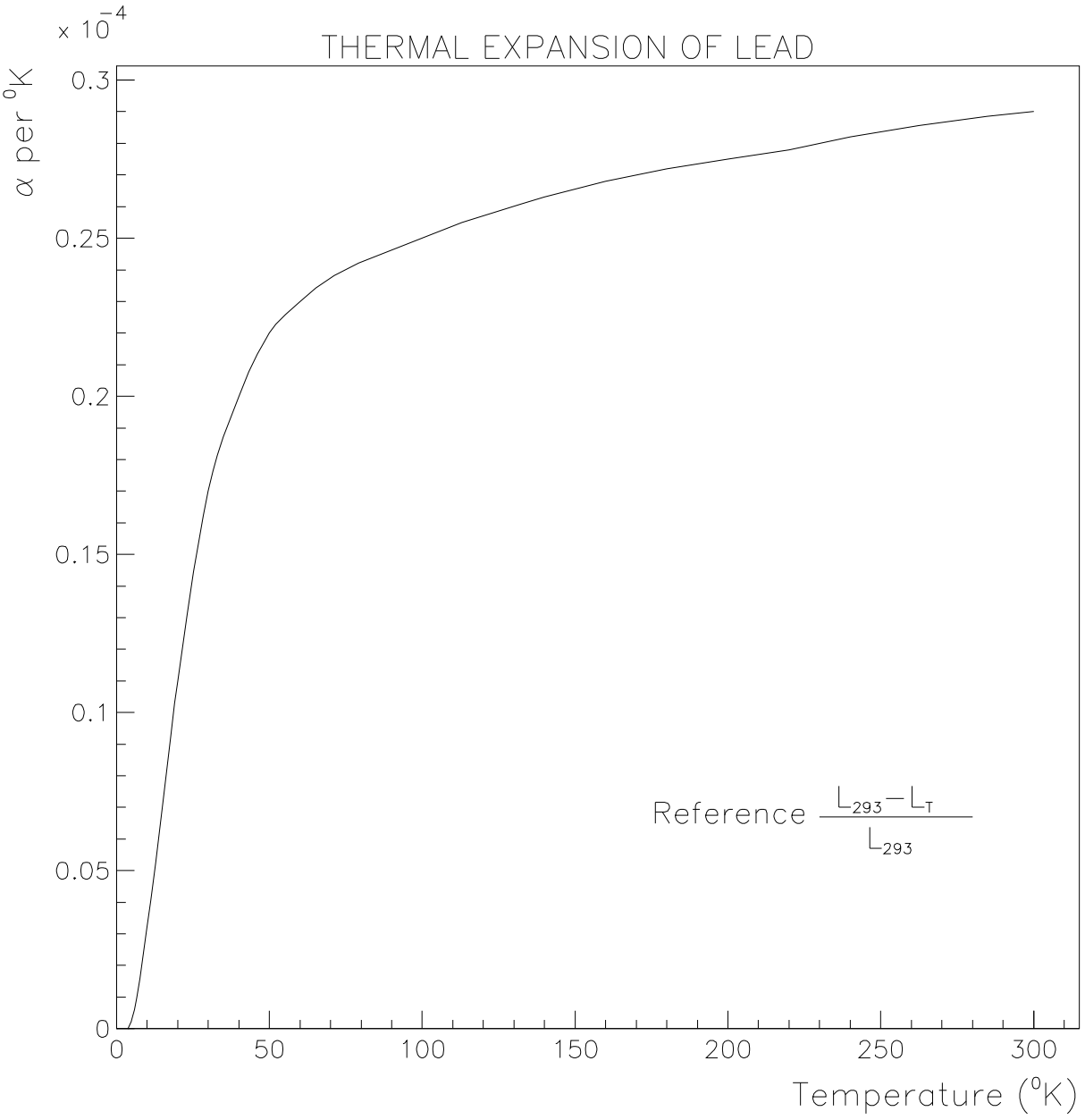
THERMAL EXPANSION OF LEAD
x 10⁻⁴
α per °K
0.3
0.25
0.2
0.15
0.1
0.05
0
0
50
100
150
200
250
300
Temperature (°K)
Reference (L293 − LT) / L293

inner model

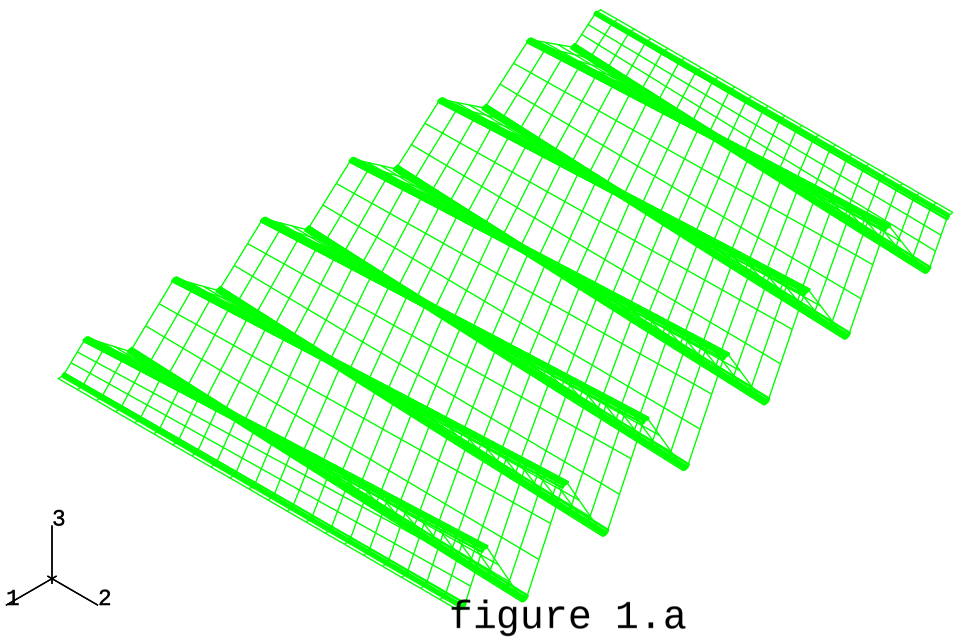

figure 1.a

outer model

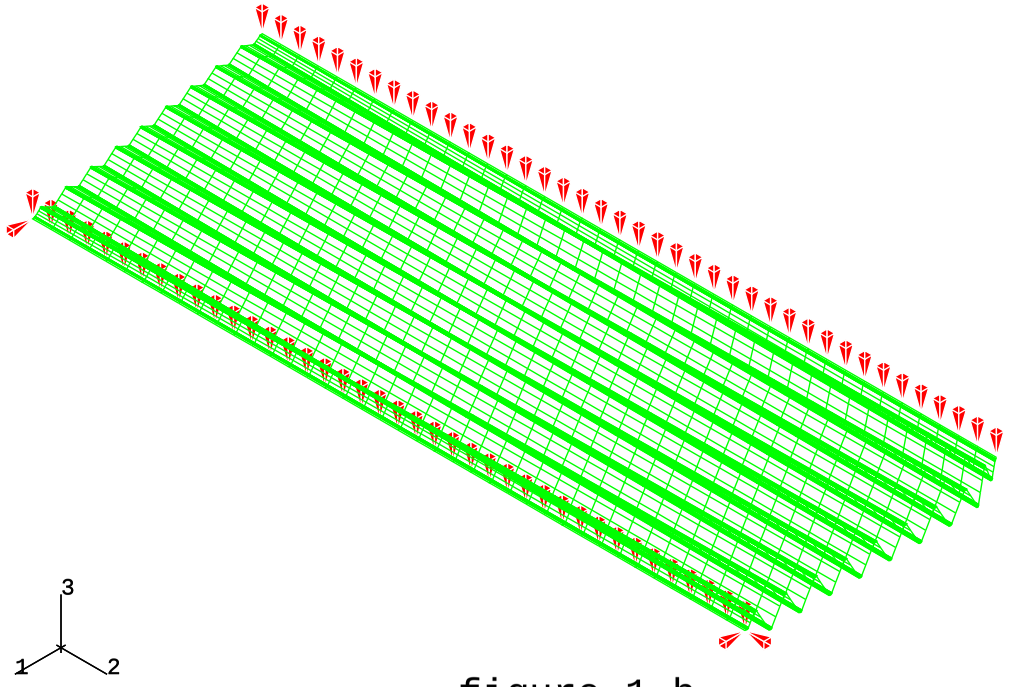

figure 1.b

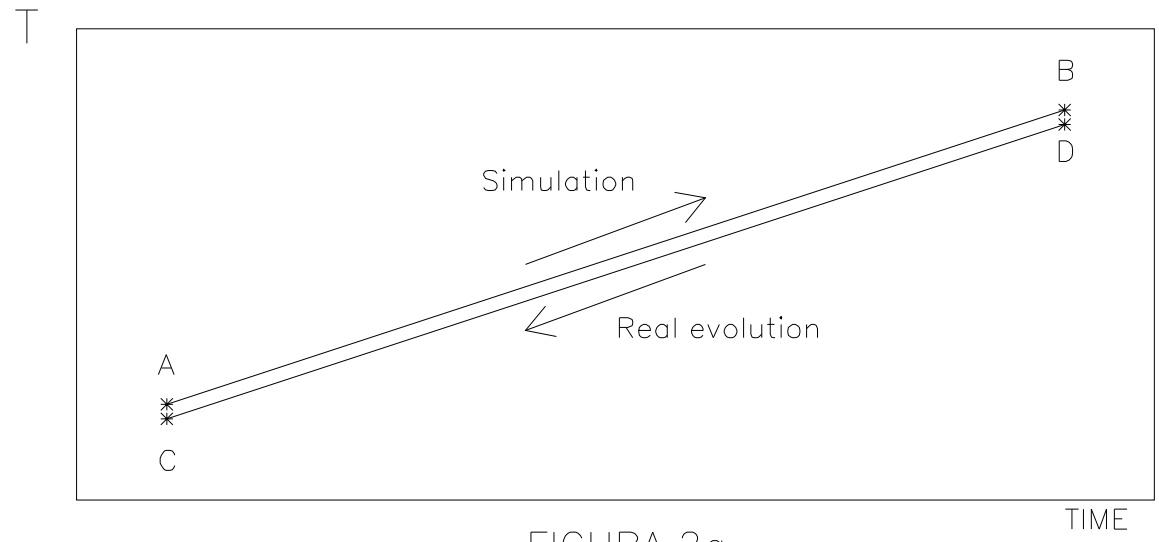

FIGURA 2a

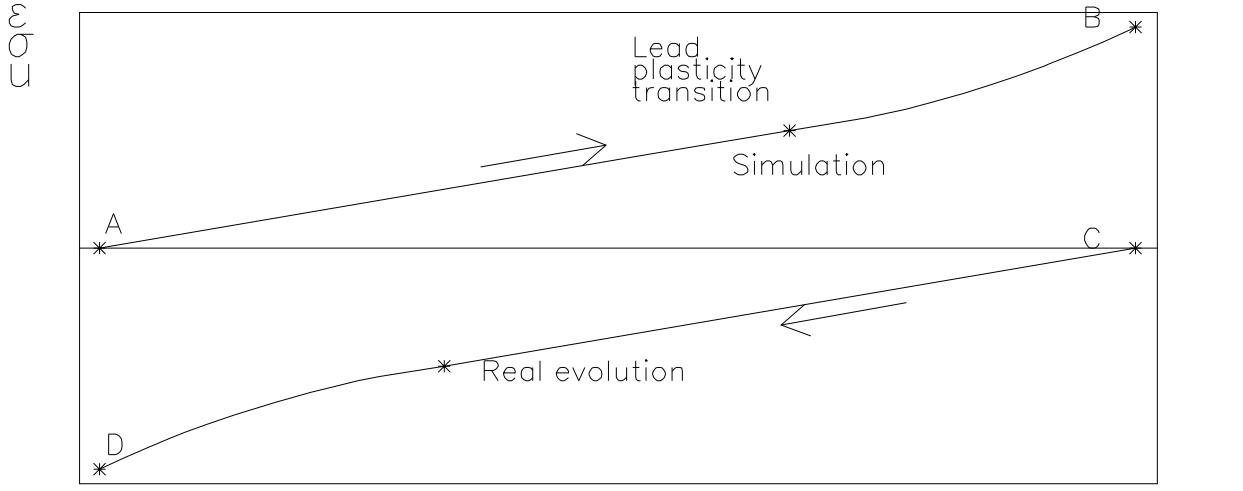

FIGURA 2b

inner/shell-solid/plastic/model

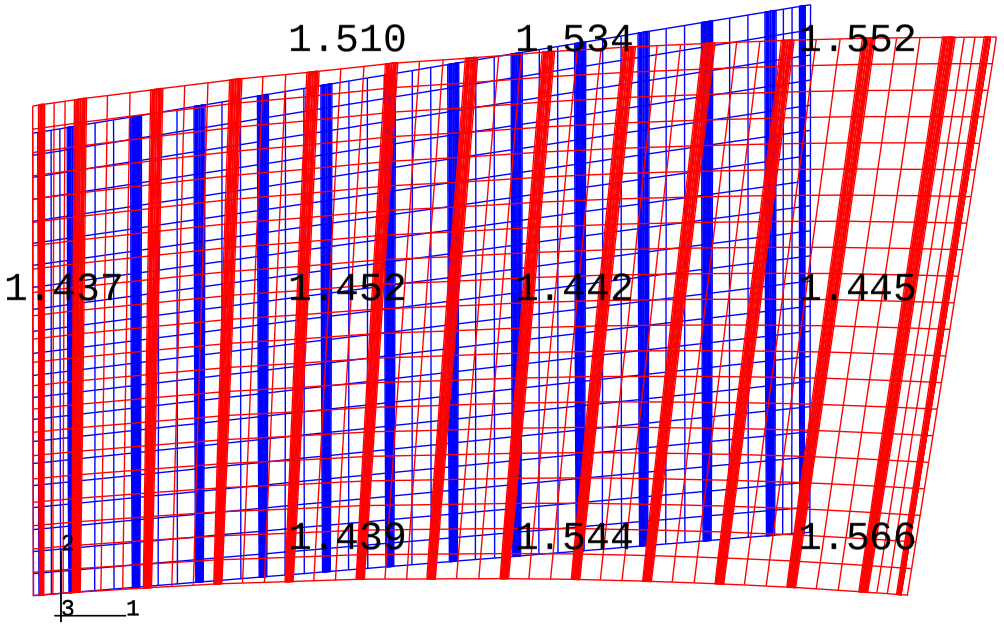

figure 3.a

inner/shell-solid/plastic/model

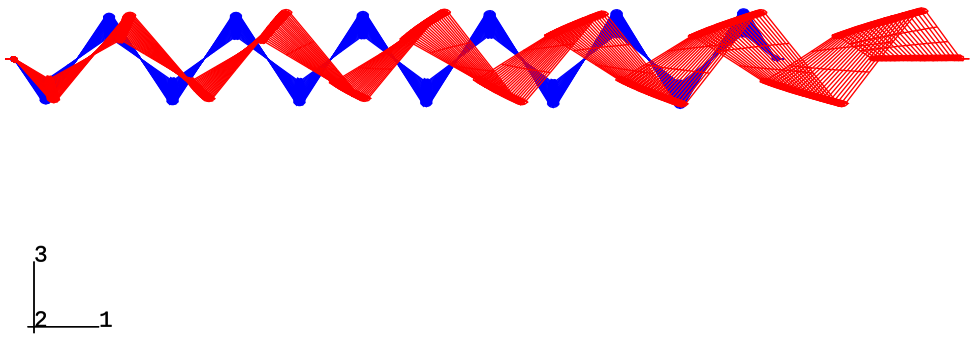

figure 3.b

outer/shell-solid/plastic/model

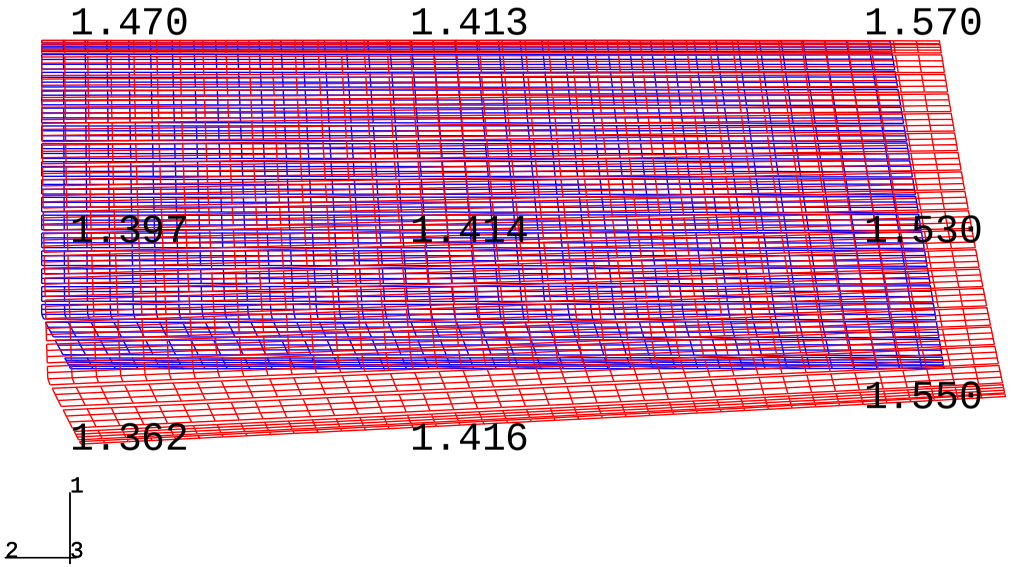

figure 4.a

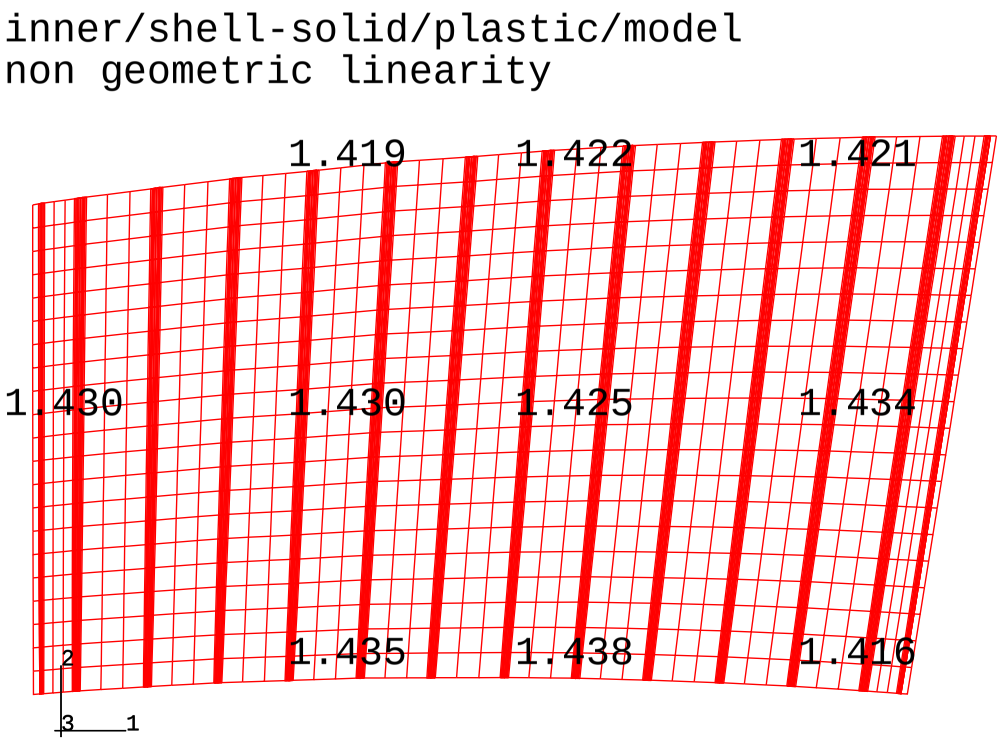
inner/shell-solid/plastic/model
non geometric linearity
1.419
1.422
1.421
1.430
1.430
1.425
1.434
1.435
1.438
1.416
2
3
1

figure 5.a

outer/shell-solid/plastic/model
non geometric linearity

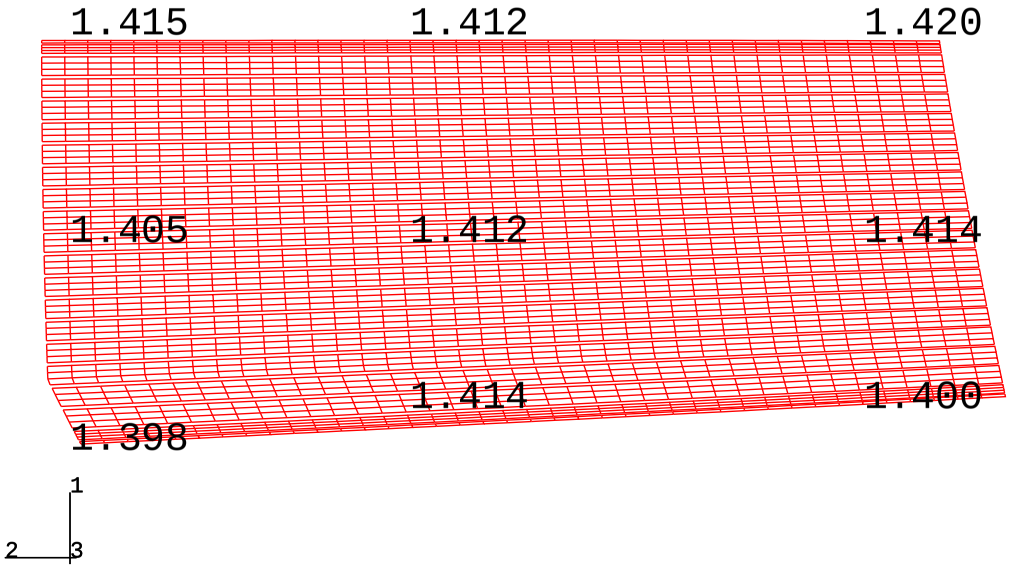

figure 5.b

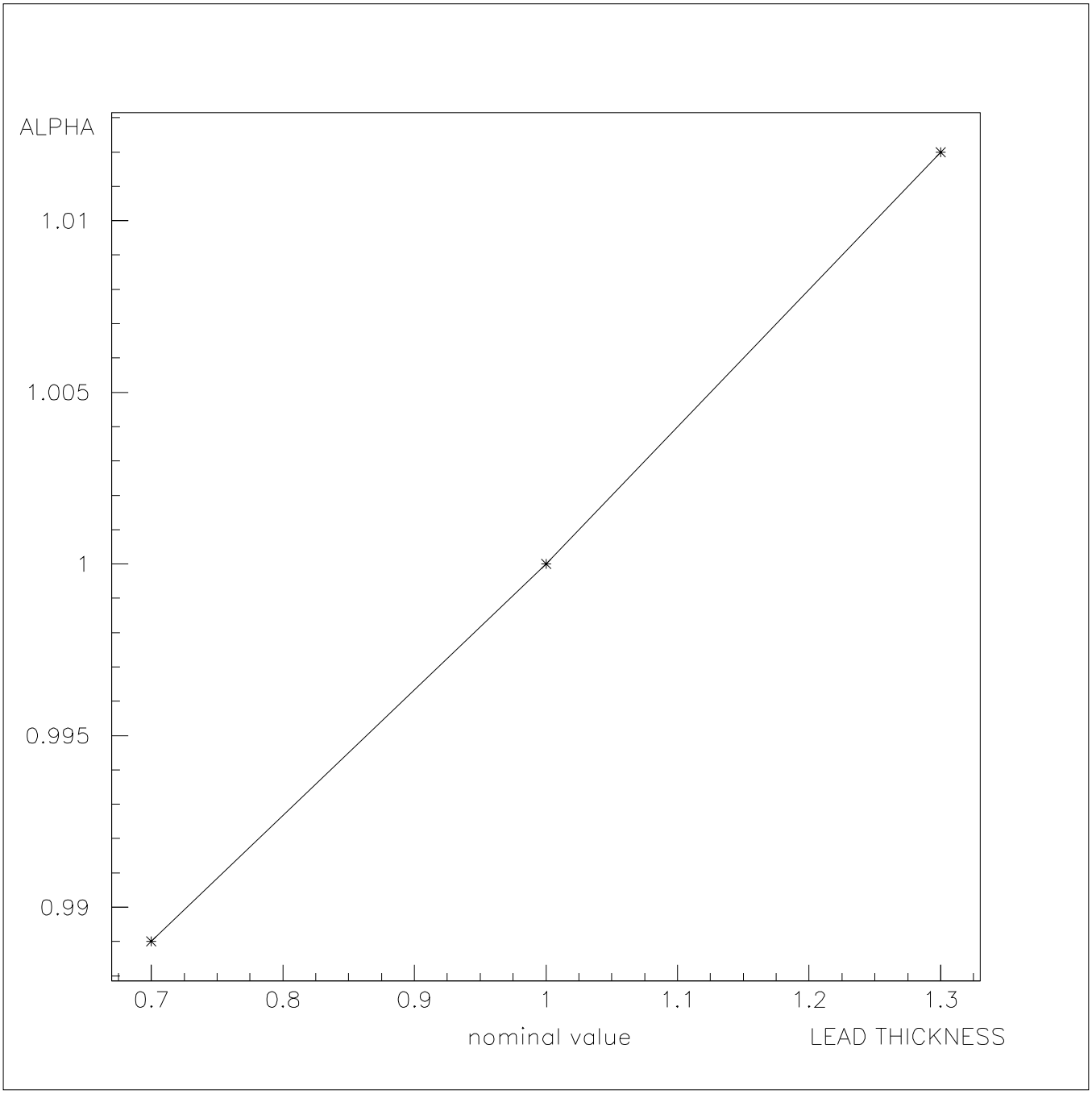
ALPHA
1.01
1.005
1
0.995
0.99
0.7
0.8
0.9
1
1.1
1.2
1.3
nominal value
LEAD THICKNESS